

# Effect of Controlled Rolling on Texture Development in a Plain Carbon and a Nb Microalloyed Steel

R. K. RAY,<sup>1)</sup> M. P. BUTRÓN-GUILLÉN, J.J. JONAS and G. E. RUDDLE<sup>2)</sup>

Department of Metallurgical Engineering, McGill University, 3450 University Street, Montreal, Quebec H3A 2A7, Canada.  
 1) Department of Metallurgical Engineering, Indian Institute of Technology, Kanpur 208016, India. 2) Department of Energy, Mines and Resources, CANMET, 568 Booth Street, Ottawa, Ontario K1A 0G1, Canada.

(Received on August 12, 1991; accepted in final form on November 15, 1991)

The effect of finish rolling temperature was investigated on texture formation in a plain C and a 0.034% Nb microalloyed steel. When finish rolled at 1020°C (*i.e.* within the  $\gamma$  recrystallization range), the textures in both steels contain the  $\{001\}\langle 110 \rangle$  and  $\{110\}\langle 110 \rangle$  components. The sharpness of the  $\{001\}\langle 110 \rangle$  component generally increases with decreasing finish rolling temperature down to 630°C, while the  $\{110\}\langle 110 \rangle$  component gradually weakens and finally disappears after ferrite rolling. The microalloyed steel displays a much sharper texture than the plain C steel when finish rolled at 870°C (*i.e.* within the  $\gamma$  pancaking range for the Nb steel) and at 730°C (in the  $\gamma + \alpha$  intercritical range). After finish rolling at 870°C, the major texture components in the microalloyed steel are  $\{113\}\langle 110 \rangle$  and  $\{332\}\langle 113 \rangle$ , in addition to the above two, while the plain C steel texture only contains some low intensity maxima. When finish rolled at 730°C, weak peaks appear at  $\{223\}\langle 110 \rangle$  and  $\{554\}\langle 225 \rangle$  in the plain C steel and stronger ones at  $\{4411\}\langle 110 \rangle$  and  $\{554\}\langle 225 \rangle$  in the microalloyed steel. After warm rolling at 630°C, the major texture components in both steels are  $\{223\}\langle 110 \rangle$ ,  $\{554\}\langle 225 \rangle$  and  $\{001\}\langle 110 \rangle$ .

The  $\{001\}\langle 110 \rangle$  and  $\{110\}\langle 110 \rangle$  components are obtained, by transformation, from the  $\{100\}\langle 001 \rangle$  (cube) and  $\{122\}\langle 212 \rangle$  (twinned cube) components of the recrystallized  $\gamma$ . By contrast, the  $\{113\}\langle 110 \rangle$  and  $\{332\}\langle 113 \rangle$  components originate, respectively, from the  $\{112\}\langle 111 \rangle$  (copper) and  $\{110\}\langle 112 \rangle$  (brass) components of the unrecrystallized  $\gamma$ . During continued rolling in the  $\gamma + \alpha$  or  $\alpha$  range, these transformation texture components are further modified by deformation and ultimately give rise to the stable end orientations which constitute the well-known warm rolling texture in steels.

KEY WORDS: controlled rolling; texture; plain C steel; microalloyed steel.

## 1. Introduction

The controlled rolling of microalloyed steels involves finishing in the unrecrystallized  $\gamma$  region. This is often followed by reductions in the intercritical ( $\gamma + \alpha$ ) and sometimes even in the upper  $\alpha$  range. When sufficient strain has accumulated in the  $\gamma$ , a fairly sharp rolling texture develops, which is later inherited by the product  $\alpha$  phase. This transformation texture is further sharpened and modified by lowering the finish rolling temperature, so that the transformed  $\alpha$  phase is also deformed.

The various kinds of transformation textures encountered in steels, their probable modes of origin and their technological importance have recently been reviewed by Ray and Jonas.<sup>1)</sup> The subject of transformation textures has taken on added significance due to the demand for low cost deep drawing steels produced directly by hot rolling for use in place of the conventional cold rolled grades. For adequate properties, such materials must possess a strong  $\{111\}$  fibre texture after transformation from the  $\gamma$ . It has also been observed that extra low carbon steels with strong  $\{111\}$  textures and therefore high  $r$ -values can be produced by rolling

in the upper  $\alpha$  range.<sup>2-6)</sup>

In spite of the technological importance of transformation textures in steels and their direct effects on mechanical properties, relatively few detailed investigations have been carried out in this area, the only systematic study to date being that of Inagaki.<sup>7-9)</sup> There is, therefore, much scope for further research on texture formation in steels during controlled rolling. The present work was undertaken with a view to determining the effect of finish rolling temperature on the development of anisotropy in a plain C and a Nb microalloyed steel. Detailed texture measurements were made on samples obtained at different stages of controlled rolling and the effect of the rolling parameters on texture formation is explained in this way.

## 2. Experimental

The chemical compositions of the two steels are given in **Table 1**. The steels were supplied by Stelco Steel in Hamilton, Canada, in the form of transfer bars about 50 mm in thickness and 1 × 1 m in size. Small ingots about 180 × 120 × 50 mm were cut from the plates and

**Table I.** Chemical compositions of the two steels. (wt%)

Steel	C	Mn	P	S	Si	Cu	Ni	Cr	Mo	V	Nb	ASA*	N
Plain C	0.20	1.24	0.011	0.004	0.185	0.012	0.013	0.030	0.006	0.004	0.002	0.044	0.0065
Nb microalloyed	0.18	1.35	0.005	0.008	0.244	0.014	0.009	0.018	0.002	0.003	0.034	0.048	0.0074

\* Acid soluble aluminum.

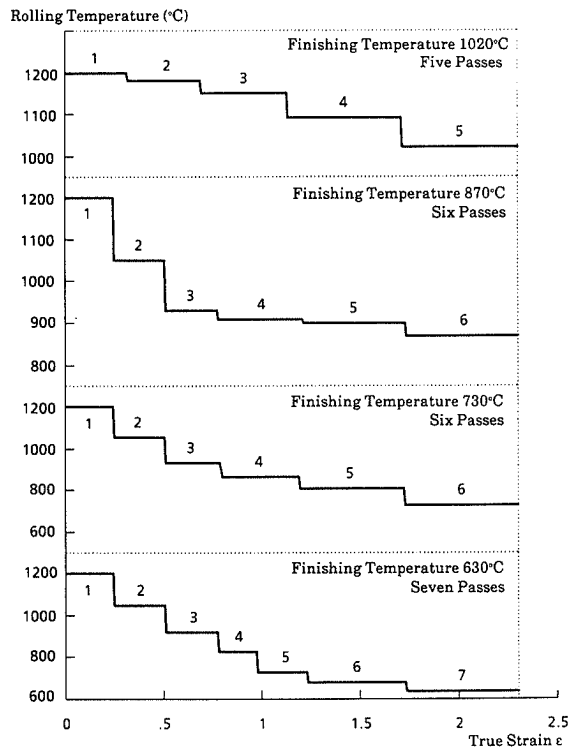


**Fig. 1.** Rolling schedules pertaining to the four finishing temperatures.

soaked for 2 h at 1250°C in an electric muffle furnace. Controlled rolling was carried out up to a total of 90% reduction in the instrumented reversing mill at CANMET, Ottawa, and rolling was initiated in each case at 1200°C. Four different rolling schedules were employed on the two steels; these involved finishing at 1020°C (in the recrystallized  $\gamma$  range), at 870°C (in the pancaked  $\gamma$  range for the Nb steel), at 730°C (in the  $\gamma + \alpha$  range) and at 630°C (in the  $\alpha$  range). The detailed rolling schedules, including the number of passes, are shown schematically in **Fig. 1**.

The rolling temperature was monitored closely by inserting thermocouples into holes drilled in the central parts of a number of trial samples of each steel. Optical pyrometers placed above the surfaces of the rolled materials were calibrated against the thermocouple readings from the centres of the samples. The calibrations were then used to record the temperature of the samples during the actual rolling operations. After rolling, all the samples were air-cooled to room temperature.

The crystallographic textures were measured in the form of  $\{110\}$ ,  $\{200\}$  and  $\{112\}$  pole figures at the sample mid-thicknesses on an automatic texture goniometer. Orientation distribution functions (ODF's) were calculated from these pole figure data in the usual manner. The texture samples were also employed for the

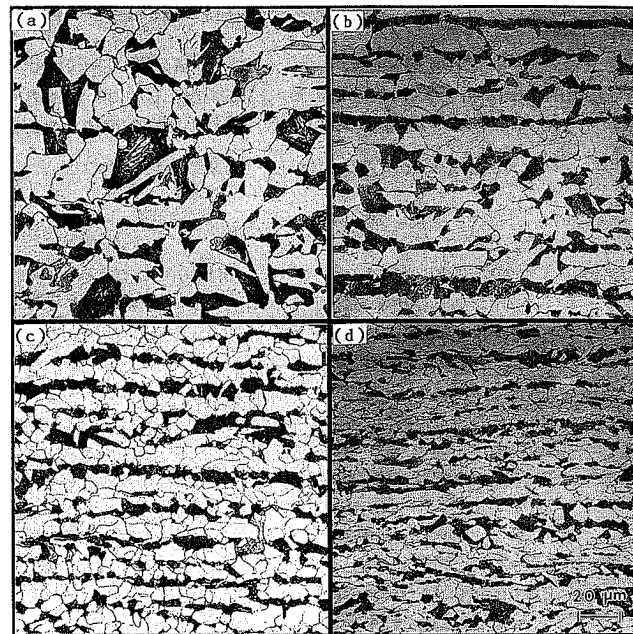


**Fig. 2.** Optical microstructures of the plain C steel, finish rolled at: (a) 1020°C, (b) 870°C, (c) 730°C and (d) 630°C.

preparation of optical micrographs.

### 3. Results

#### 3.1. Optical Microstructures

The microstructures of the plain C steel finish rolled at the four different temperatures are illustrated in **Fig. 2**. Large, nearly equiaxed ferrite grains are obtained when the steel is finished at 1020°C. These grains were produced by transformation from austenite grains formed by static recrystallization after deformation at that relatively high temperature. Finish rolling at 870 and 730°C produces progressively finer but still nearly equiaxed ferrite grains. The shape of the pearlite grains indicates that very little pancaking of the untransformed  $\gamma$  grains occurred during finish rolling at 870°C, which must be above the  $T_{nr}$  for the austenite phase in this steel. (The  $T_{nr}$  or 'no-recrystallization' temperature is that below which austenite recrystallization no longer takes place during the interpass intervals.) However, rolling in the intercritical range did produce some pearlite pancaking, which indicates that rolling was carried out below the  $T_{nr}$ . After warm rolling at 630°C, the ferrite grains appear flat and elongated, indicating that the ferrite  $T_{nr}$  is well above 630°C.

The optical microstructures of the microalloyed steel finish rolled at the same temperatures are presented in **Fig. 3**. As in the case of the plain C steel, large and approximately equiaxed ferrite grains are present in the

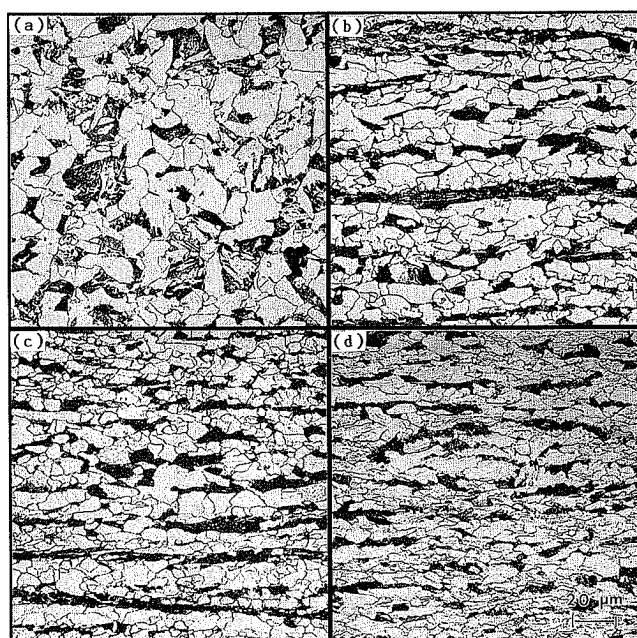


Fig. 3. Optical microstructures of the microalloyed steel, finish rolled at: (a) 1020°C, (b) 870°C, (c) 730°C and (d) 630°C.

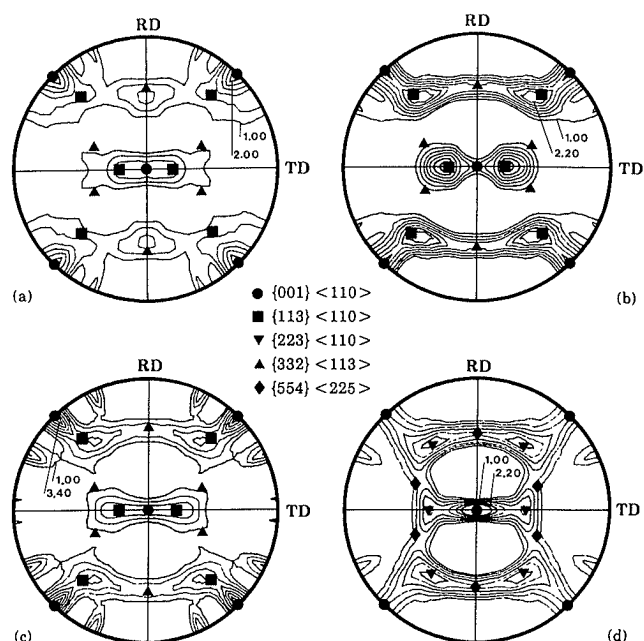


Fig. 5. (200) pole figures of the microalloyed steel, finish rolled at: (a) 1020°C, (b) 870°C, (c) 730°C and (d) 630°C.

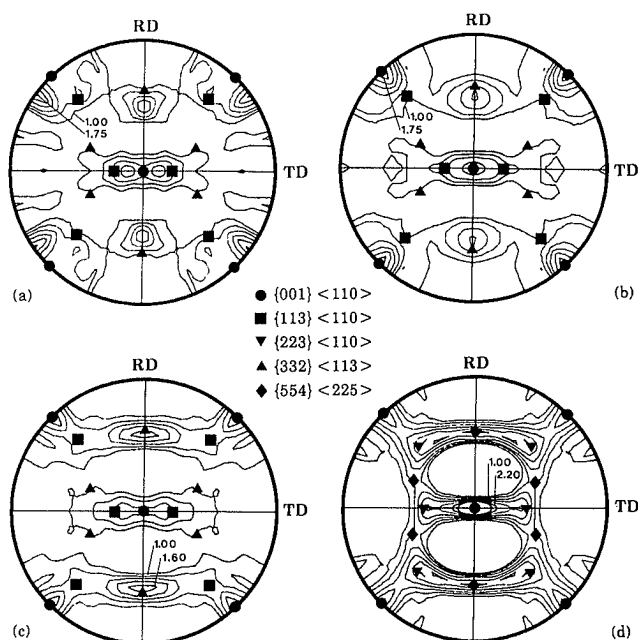


Fig. 4. (200) pole figures of the plain C steel, finish rolled at: (a) 1020°C, (b) 870°C, (c) 730°C and (d) 630°C.

specimen finish rolled at 1020°C. Finish rolling at 870 and 730°C produces a progressively finer ferrite grain size and the shape of the pearlite grains indicates that the untransformed  $\gamma$  grains were being pancaked. After rolling at the latter temperature, which is below the ferrite  $T_m$ , elongated  $\alpha$  grains can be seen. This is due to the presence of Nb in this steel. After warm rolling at 630°C, deformed and elongated ferrite grains appear, as in the case of the plain C steel.

### 3.2. Pole Figures and ODF's

The (200) pole figures for the plain C steel finish rolled

at the four different temperatures are shown in Fig. 4. These are complete pole figures recalculated from the corresponding ODF's. The locations of a few ideal orientations have been marked in each of these diagrams. Figures 4(a) to 4(c) display many similarities; all are rather weak in intensity (the highest intensity is 1.9 times random) and have similar pole distributions. The most clearly identified orientation is the {001}<110>. The maxima are slightly shifted from this ideal orientation to {001}<230> in Fig. 4(a). A somewhat sharper texture is obtained after ferrite rolling (Fig. 4(d)). Here the texture components appear as {001}<110>, {554}<225> and {223}<110>, all of moderately strong intensity.

The (200) pole figures for the microalloyed steel finish rolled at the four different temperatures are presented in Fig. 5. Comparison with those for the plain C steel (see Fig. 4) indicates that the microalloyed ones are detectably more intense. Although the pole distribution patterns in Figs. 4(a) and 5(a) are similar, the differences are greater between Figs. 4(b) and 4(c) on the one hand and Figs. 5(b) and 5(c) on the other. The major orientations present in the textures of the Nb steel finish rolled at 870 and 730°C are the {001}<110> and {113}<110>. The texture of the microalloyed steel after ferrite rolling (see Fig. 5(d)) is almost identical to the texture of the similarly treated plain C steel (see Fig. 4(d)).

The  $\phi_1 = 0^\circ$  and  $\phi_1 = 90^\circ$  sections of the experimental ODF's for the plain C and the microalloyed steel are shown in Figs. 6 and 7, respectively. Figure 6 again indicates that the overall intensities of the plain C textures are low for finishing temperatures of 1020, 870 and 730°C. However, the sharpness increases significantly after ferrite rolling at 630°C. In all cases, the major texture component is the {001}<110>. In the sample finished at 1020°C, there is also a strong component at {110}<110>. The intensity of the latter decreases as the finish rolling temperature is lowered and it disappears

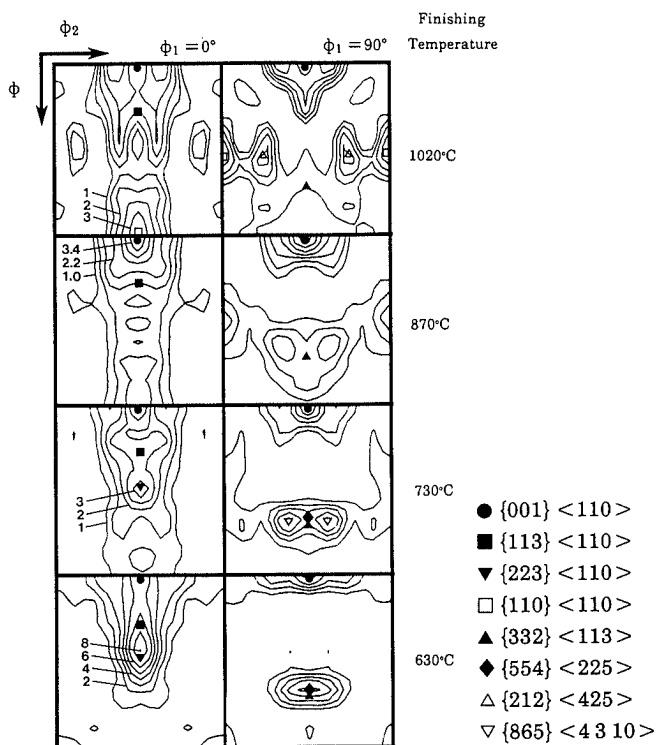


Fig. 6. The  $\phi_1 = 0^\circ$  and  $\phi_1 = 90^\circ$  sections of the experimental ODF's of the plain C steel.

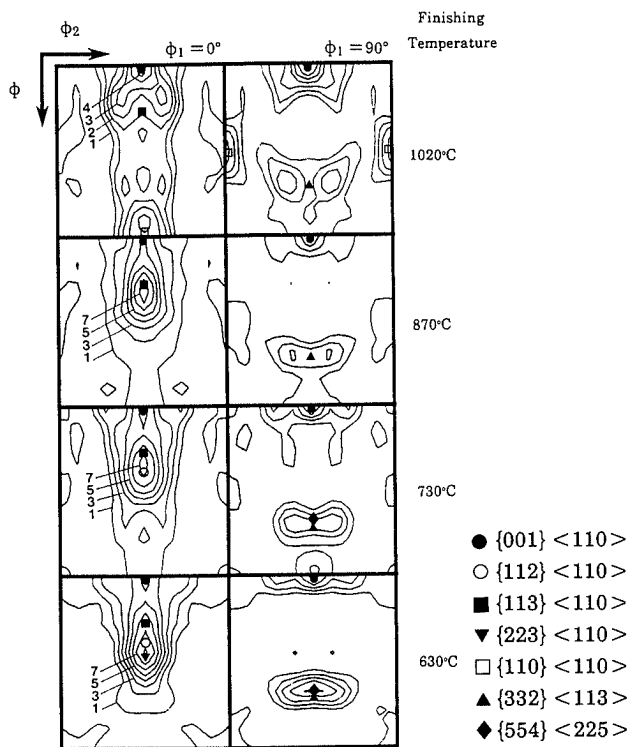


Fig. 7. The  $\phi_1 = 0^\circ$  and  $\phi_1 = 90^\circ$  sections of the experimental ODF's of the microalloyed steel.

completely after ferrite rolling. A component near  $\{865\}\langle 4310 \rangle$  (which is close to  $\{332\}\langle 113 \rangle$ ) appears in the texture of the sample finish rolled at  $870^\circ\text{C}$  and its intensity increases when the finishing temperature is lowered to  $730^\circ\text{C}$ . Finally, after ferrite rolling, the  $\{332\}\langle 113 \rangle$  is displaced to become a strong  $\{554\}\langle 225 \rangle$  component. The  $\{223\}\langle 110 \rangle$  orientation appears as an

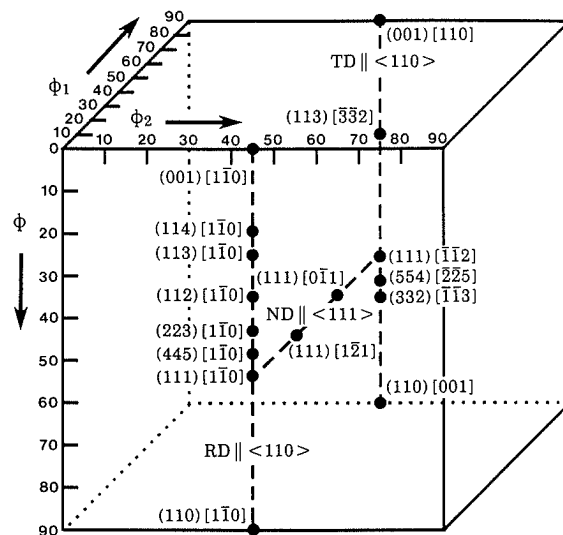


Fig. 8. A three-dimensional view of Euler space, showing the locations of important orientations belonging to the RD, TD and ND fibres.

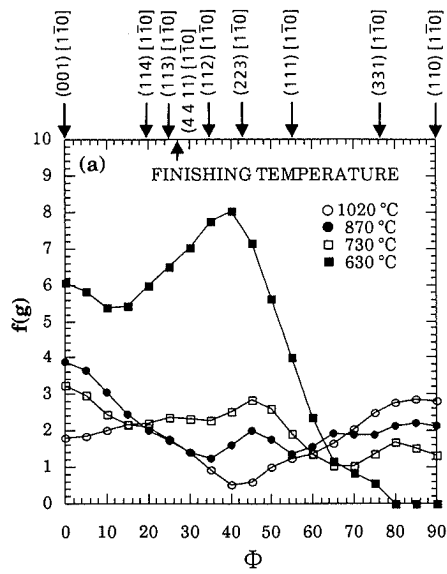
important texture component in the sample finished at  $730^\circ\text{C}$  and this becomes the strongest orientation after ferrite rolling.

Figure 7 shows that the microalloyed steel textures are much sharper than those of the plain C steel. Here, as before,  $\{001\}\langle 110 \rangle$  and  $\{110\}\langle 110 \rangle$  are the two most important components in the sample finish rolled at  $1020^\circ\text{C}$ . In addition, there is a moderately strong  $\{865\}\langle 4310 \rangle$  component, which is not very far from  $\{332\}\langle 113 \rangle$ . As the finish rolling temperature is decreased, the overall intensity of the texture sharpens significantly (by a factor of 1.5 to 2 times). For the specimen finish rolled at  $870^\circ\text{C}$ , the major texture component is located near the  $\{113\}\langle 110 \rangle$ . This is also the main texture component for the steel finished at  $730^\circ\text{C}$ . After ferrite rolling, the major texture component shifts to  $\{223\}\langle 110 \rangle$ , while the other components are  $\{554\}\langle 225 \rangle$  and  $\{001\}\langle 110 \rangle$ .

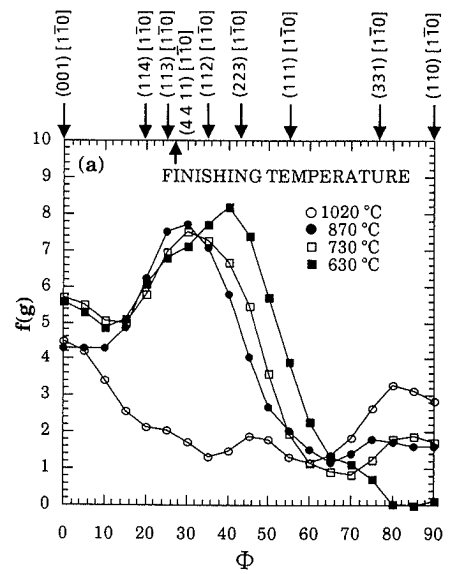
### 3.3. RD, TD and ND Fibres

The three important fibres which are normally used to describe the textures in rolled and recrystallized ferrite are represented in Euler (ODF) space in Fig. 8. These are referred to here as the RD, ND and TD fibres. Although the Greek letters,  $\alpha$ ,  $\gamma$  and  $\epsilon$  have been used by Seidal *et al.*<sup>10)</sup> to denote these fibres, that terminology is not adopted in this paper in order to avoid confusion with the  $\alpha$  and  $\gamma$  phases in steels. All the orientations lying along the RD fibre are related by rotations along the RD  $\parallel \langle 110 \rangle$  axis, and the fibre lies along  $\phi_2 = 45^\circ$  in the  $\phi_1 = 0^\circ$  section. Orientations on the ND fibre have a common  $\langle 111 \rangle \parallel \text{ND}$  and this fibre extends parallel to the  $\phi_1$  axis at  $\phi = 55^\circ$  and  $\phi_2 = 45^\circ$ . The TD fibre contains orientations that have a common  $\langle 110 \rangle \parallel \text{TD}$  and this fibre lies along  $\phi_2 = 45^\circ$  in the  $\phi_1 = 90^\circ$  section.

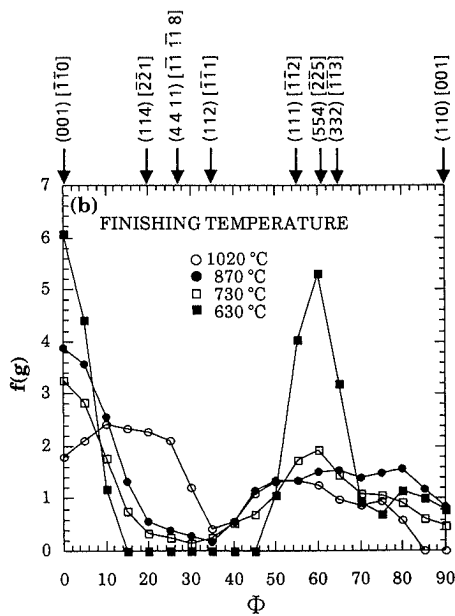
The differences between the textures of the two steels can be recognized more clearly when the relevant data are plotted in terms of these fibres. The plain C pole density  $f(g)$  distribution along the RD fibre is shown in Fig. 9(a). When finish rolled at  $1020^\circ\text{C}$ , this steel displays



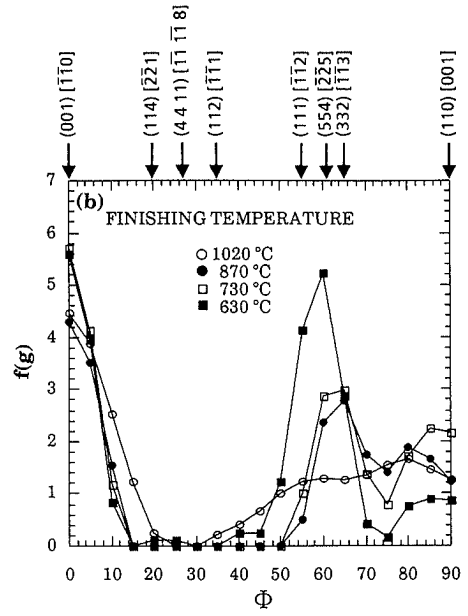
(a)  $f(g)$  vs.  $\Phi$  along the RD fibre



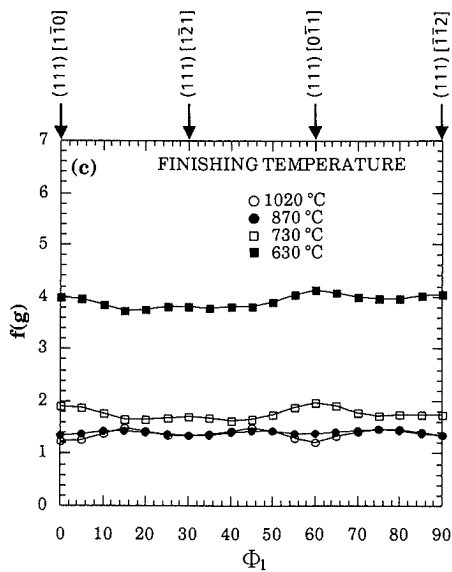
(a)  $f(g)$  vs.  $\Phi$  along the RD fibre



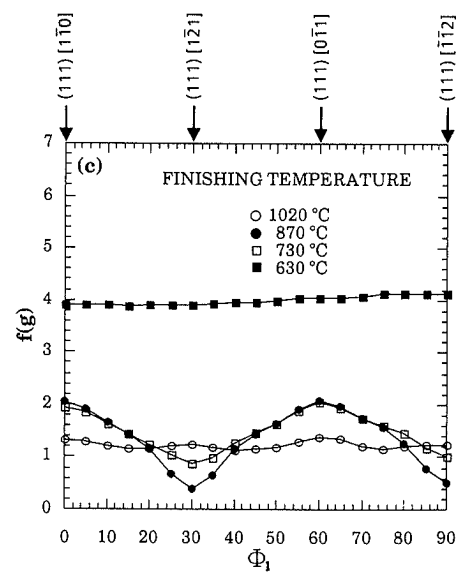
(b)  $f(g)$  vs.  $\Phi$  along the TD fibre



(b)  $f(g)$  vs.  $\Phi$  along the TD fibre



(c)  $f(g)$  vs.  $\Phi_1$  along the ND fibre



(c)  $f(g)$  vs.  $\Phi_1$  along the ND fibre

Fig. 9. For the plain C steel.

Fig. 10. For the microalloyed steel.

moderate values (2.0 to 3.0) of  $f(g)$  at and around (001)[110] and (110)[110]. On lowering the finishing temperature first to 870°C and then to 730°C (the latter is within the  $\gamma + \alpha$  intercritical range), the (001)[110] intensity is sharpened progressively while the (110)[110] is decreased. In addition, a small intensity hump appears near (223)[110]. Finish rolling in the  $\alpha$  range (at 630°C) causes a drastic change in the nature as well as the overall intensity of the RD fibre; it now displays a sharp texture component, lying between (112)[110] and (223)[110]. This is accompanied by a sharp increase in the intensity of the (001)[110] orientation, while the (110)[110] component totally disappears.

An examination of the TD fibre for the plain C steel finish rolled at 1 020°C (Fig. 9(b)) reveals a broad intensity maximum centred around (114)[221], in addition to the presence of the (001)[110] orientation. On lowering the finishing temperature to 870°C, the (001)[110] intensity sharpens considerably and the hump around (114)[221] disappears. By contrast, a small peak near (554)[225] appears after finish rolling at 730°C. The intensity of this peak shows a drastic increase and the (001)[110] component is further sharpened by ferrite rolling (at 630°C).

The ND fibres for the plain C steel are presented in Fig. 9(c). The orientation densities are relatively constant along this fibre in the samples finished at the four different temperatures. While the orientation densities of the fibres corresponding to finishing temperatures of 1 020 and 870°C are slightly above random, the  $f(g)$  for the 730°C finished material is about 2 times random. Ferrite rolling (at 630°C) produces an ND fibre with the highest  $f(g)$  value, nearly 4.0.

Comparison of the RD and TD plots for the plain C steel (Figs. 9(a) and 9(b)) with those for the microalloyed steel (Figs. 10(a) and 10(b)) reveals that the texture components in the latter are decidedly more intense than in the former. The RD plot for the Nb steel (Fig. 10(a)) finish rolled at 1 020°C displays higher intensities of the (001)[110] and (110)[110] components, a small hump near (223)[110], plus a moderately intense peak at (331)[110]. Lowering the finish rolling temperature to 870°C causes a drastic increase in the intensities of the components between (114)[110] and (223)[110]. Furthermore, a sharp peak appears close to the (113)[110] orientation, the intensity of the (001)[110] component remains practically unchanged, and that of the (110)[110]

is weakened. On decreasing the finish rolling temperature to 730°C, the (113)[110] peak is shifted to near (4 4 11)[110] and the (001)[110] component is sharpened, while (110)[110] remains practically unchanged. Finishing in the ferrite range (630°C) shifts the peak of the RD fibre to near (223)[110] and also increases its intensity slightly. At the same time, the (110)[110] component disappears completely.

The TD fibre for the Nb steel (Fig. 10(b)) finish rolled at 1 020°C displays, in addition to the sharp (001)[110] component, a low intensity plateau ranging from (111)[112] to (110)[001]. This intensity sharpened significantly and showed a maximum at (332)[113] when finish rolling was carried out at 870°C. This peak is sharpened further when the finish rolling temperature is lowered to 730°C. There is also some increase in the strengths of the (001)[110] and (110)[001] components at this stage. After ferrite rolling (630°C), there is a perceptible shift of the (332)[113] component to (554)[225], which also has a much higher intensity. At the same time the (110)[001] drops to below random.

The ND fibres for the microalloyed steel (Fig. 10(c)) show surprising similarities to the corresponding plots for the plain C steel (Fig. 9(c)). While the fibre of the sample finish rolled in the  $\gamma$  recrystallization range (1 020°C) is of nearly uniform intensity, those for the 870 and 730°C finished materials display perceptible increases in the intensities of the  $\{111\}\langle 110 \rangle$  component and a corresponding decrease in the intensities of the  $\{111\}\langle 112 \rangle$  component. A reasonably strong ND fibre of remarkably uniform intensity ( $f(g)=4.0$ ) is obtained after ferrite rolling at 630°C.

The texture components observed experimentally at different stages of controlled rolling in the two steels are compared in Table 2. The formation of these components and the modifications they undergo during rolling will now be considered in more detail.

#### 4. Discussion

The above results indicate that the textures of plain C and Nb microalloyed steels are similar when these are either finish rolled in the  $\gamma$  recrystallization range (at 1 020°C) or are subjected to warm (ferrite) rolling. By contrast, when finish rolling is carried out at 870°C (which is in the  $\gamma$  recrystallization range for the C steel, but in the  $\gamma$  no-recrystallization range for the Nb steel) as well

Table 2. Effect of finish rolling temperature on major texture components in the C and the Nb steel.

Steel	Texture components observed after finish rolling at				Changes in intensity with lowering of finish rolling temperature
	1 020°C	870°C	730°C	630°C	
Plain C	{001}<110>	{001}<110>	{001}<110>	{001}<110>	Generally sharpens Generally weakens Sharpens remarkably Sharpens remarkably
	{110}<110>	{110}<110>	{110}<110>	{110}<110>	
			{223}<110>	{223}<110>	
			{554}<225>	{554}<225>	
Nb microalloyed	{001}<110>	{001}<110>	{001}<110>	{001}<110>	Generally sharpens Generally weakens Generally sharpens Sharpens
	{110}<110>	{110}<110>	{110}<110>	{110}<110>	
		{113}<110>→	{4 4 11}<110>→	{223}<110>	
		{332}<113>→	{554}<225>	{554}<225>	

**Table 3.** bcc orientations derived from orientations in fcc  $\gamma$ .

Initial fcc orientation*	Derived bcc orientation
{100}<001> (cube)	{001}<110>
	{110}<001>
	{110}<110>
{122}<212> (twinned cube)	{001}<110>
	{110}<001>
	{110}<110>
{110}<112> (Bs)	{332}<113>
	{111}<112>
	{001}<110>
{112}<111> (Cu)	{113}<110>
	{112}<110>
	{201}<102>
	{110}<110>
{123}<634> (S)	{113}<110>
	{332}<113>
	{110}<110>

\* The cube, Bs, Cu and S orientations are defined and described in more detail in Ref. 1).

as in the  $\gamma + \alpha$  intercritical range (at 730°C), the two steels respond very differently with regard to texture formation. This is because the deformation textures acquired by the Nb steel during rolling are subsequently inherited by the product phase ( $\alpha$ ) after transformation. Although experimental difficulties generally preclude the direct measurement of  $\gamma$  hot rolling textures, these have been successfully simulated through the use of fcc materials with comparable stacking fault energies (SFE's). For example, an alloy of Ni with 30 wt% cobalt has an SFE similar to that of  $\gamma$  iron, and has been employed successfully as a model material for simulation purposes.<sup>11)</sup>

In this way, the major components of the  $\gamma$  rolling textures have been shown to be the {110}<112> (Bs), {112}<111> (Cu) and {123}<634> (S); similarly, the main recrystallization texture components are the {100}<001> (cube) and {122}<212> (twinned cube). These austenite texture components and the ferrite orientations that are obtained from them are summarized in **Table 3**.<sup>12)</sup>

#### 4.1. Similarities between the Textures of the C and the Nb Steel

After finish rolling at 1020°C, the major texture component in both the plain C and the microalloyed steel is {001}<110>. This is obtained from the *recrystallized*  $\gamma$  in the form of a strong cube component, {100}<001>, and its twin, {122}<212>. The other important component present in the two steels at this stage, namely the {110}<110>, can also be derived from the above two components of recrystallized  $\gamma$  (see **Table 3**).

The {001}<110> orientation is an important component of the transformation texture in both steels, even after finish rolling at 870 and 730°C, and, in case of the C steel, it is perceptibly sharper at these lower temperatures than when the specimens are finish rolled at 1020°C. Finish rolling at 870°C rather than 1020°C (both temperatures are in the  $\gamma$  recrystallization range for the C steel) leads to more accumulated strain prior

to each cycle of recrystallization. This appears to produce a sharper cube texture in the austenite and therefore a more severe {001}<110> component in the transformed  $\alpha$ .

By contrast, in the microalloyed steel the presence of Nb appears to strengthen the recrystallization (*i.e.* the cube) component in the  $\gamma$ . This causes the {001}<110> component to be sharper after finish rolling at 1020°C. Lowering the finish rolling temperature to 870°C (which is in the  $\gamma$  *no-recrystallization range* for the Nb steel) decreases the amount of cube oriented material in the  $\gamma$  and therefore leads to a weakening of the {001}<110> component in the ferrite. The subsequent sharpening of this orientation, after finish rolling at 730°C (in the  $\gamma + \alpha$  intercritical range), is due to the effect of  $\alpha$  rolling. The slight decrease in the strength of this component in the C steel after finish rolling at 730°C may be due to recrystallization of the ferrite. The lack of any ferrite pancaking in this material, at this stage of rolling points to this possibility (see **Fig. 2**).

The present results also show that ferrite rolling increases the sharpness of the {001}<110> component in both steels. This indicates that it is both highly stable and amenable to further sharpening by deformation in the  $\alpha$  region. These results are in conflict with Inagaki and Suda's observations<sup>13)</sup> that this ferrite orientation lacks stability and that, on deformation, its intensity decreases while the peak is shifted along the RD fibre to close to {114}<110>. However, the present results are in good agreement with those of some recent experiments by Lücke and co-workers,<sup>10,14)</sup> and are also supported by the deformation texture simulations of Tóth *et al.*<sup>15)</sup>

The other important orientation observed in both steels after finish rolling at 1020°C is the {110}<110>. This component decreases almost continuously in intensity as the finish rolling temperature is lowered in the  $\gamma$  and  $\gamma + \alpha$  ranges and finally disappears after ferrite rolling. As shown by the texture simulations of Tóth *et al.*,<sup>15)</sup> the {110}<110> orientation in ferrite is highly unstable during rolling, and there is an orientation flow from this position towards {111}<110>. Thus, the disappearance of the {110}<110> component is expected to enhance the ND fibre simultaneously, which is precisely what is observed, in both steels after ferrite rolling.

#### 4.2. Differences in the Textures of the C and the Nb Steel

Significant differences in the transformation textures of the plain C and Nb steels were noted when finish rolling was carried out at 870°C. In the microalloyed steel, the precipitation of NbCN leads to the suppression of recrystallization in the  $\gamma$ , thereby producing a sharp  $\gamma$  rolling texture.<sup>1)</sup> As a result, a marked  $\alpha$  texture is produced after transformation. The  $\alpha$  texture in this material consists of a distinct component in the vicinity of {113}<110> and another near {332}<113>. These are primarily derived, respectively, from the {112}<111> and {110}<112> components of the unrecrystallized  $\gamma$ . By contrast, a much weaker and flatter texture is present in the plain C steel at this stage because the recrystallization of  $\gamma$  could not be suppressed. The optical microstructures of the two steels at this stage

(Figs. 2 and 3) support this view; while the plain C steel consists of nearly equiaxed and larger ferrite grains, finer grains, some equiaxed and some elongated and flat, constitute the structure of the microalloyed steel.

The sharp differences between the textures of the two steels are maintained even after finish rolling at 730°C (*i.e.* in the  $\gamma + \alpha$  intercritical range). In contrast to the previous cases, the texture of the  $\alpha$  at this stage includes contributions from (i) texture development in the parent  $\gamma$  phase, (ii) the effects of the  $\gamma \rightarrow \alpha$  transformation, and (iii) texture development in the product  $\alpha$  phase. In addition to the  $\{001\}\langle 110 \rangle$ , the two major components of the plain C steel texture are the  $\{223\}\langle 110 \rangle$  and  $\{554\}\langle 225 \rangle$ , while the corresponding orientations in the microalloyed steel are near  $\{4411\}\langle 110 \rangle$  and  $\{332\}\langle 113 \rangle / \{554\}\langle 225 \rangle$ .

The two transformation texture components in the microalloyed steel can be construed as having been formed from the  $\{112\}\langle 111 \rangle$  and  $\{110\}\langle 112 \rangle$  components, respectively, of the deformed  $\gamma$ . However, when compared to the texture of the 870°C finished material, there is a perceptible shift in the maxima of the two components in the directions:  $\{113\}\langle 110 \rangle \rightarrow \{4411\}\langle 110 \rangle$  and  $\{332\}\langle 113 \rangle \rightarrow \{554\}\langle 225 \rangle$  (see Figs. 10(a) and 10(b)). These two shifts correspond to increasing  $\Phi$  along the RD fibre and decreasing  $\Phi$  along the TD fibre, respectively.

The locations of the two major components of the plain C steel texture, namely,  $\{223\}\langle 110 \rangle$  and  $\{554\}\langle 225 \rangle$ , show a much larger shift along the above two directions and away from the positions of the ideal components derived from the unrecrystallized  $\gamma$  texture (see Figs. 9(a) and 9(b)). Tóth *et al.*,<sup>15)</sup> in their simulations of texture development in ferrite during rolling, have shown that the  $\{223\}\langle 110 \rangle$  and  $\{554\}\langle 225 \rangle$  orientations are much more stable, respectively, than the  $\{113\}\langle 110 \rangle$  and  $\{332\}\langle 113 \rangle$ . Since finish rolling in the  $\gamma + \alpha$  range involves the rolling of transformed  $\alpha$ , the displacements of the  $\{113\}\langle 110 \rangle$  and  $\{332\}\langle 113 \rangle$  orientations along the above-mentioned directions is to be expected. Before finish rolling in the  $\gamma + \alpha$  range, the microalloyed steel already had a fairly sharp  $\gamma$  deformation texture. Thus the contribution from the rolling of whatever  $\alpha$  formed in the intercritical range is not significant enough to cause a major shift in orientation of the texture components. By contrast, the plain C steel only possessed a weak  $\gamma$  deformation texture to begin with, so that the relative contribution of  $\alpha$  rolling in the  $\gamma + \alpha$  range to the overall ferrite texture is significant enough to produce a larger shift in the ideal texture components derived from the unrecrystallized  $\gamma$ .

#### 4.3. Warm Rolling Textures of the C and the Nb Steel

The plain C and Nb steel textures were remarkably similar after warm rolling at 630°C. In addition to the strong  $\{001\}\langle 110 \rangle$  component, both steels contain two other highly intense components, *i.e.* the  $\{223\}\langle 110 \rangle$  and  $\{554\}\langle 225 \rangle$ . As discussed earlier, the  $\{223\}\langle 110 \rangle$  portion of the RD fibre is more stable than the  $\{113\}\langle 110 \rangle$ , while the  $\{554\}\langle 225 \rangle$  portion of the TD fibre is more stable than the  $\{332\}\langle 113 \rangle$ .<sup>15)</sup> As a result, during  $\alpha$  rolling,

there is a net orientation flow from  $\{113\}\langle 110 \rangle$  towards  $\{223\}\langle 110 \rangle$  and from  $\{332\}\langle 113 \rangle$  towards  $\{554\}\langle 225 \rangle$ . Evidently, deformation of the  $\alpha$  plays a much more important role in texture formation in the plain C steel than the transformation of the  $\gamma$  deformation texture inherited by the  $\alpha$ . Thus, although a weak texture was produced by finish rolling at 730°C, further rolling down to 630°C led to the formation of a much stronger texture. In the microalloyed steel, on the other hand,  $\alpha$  rolling produced only a moderate sharpening of the existing texture plus some displacement of the components to more stable orientations.

The results indicate that the formation of warm rolling textures is only slightly influenced by the initial transformation texture inherited by the  $\alpha$  from the  $\gamma$ . This is further supported by the observation that an almost perfect ND fibre of about the same strength is formed in both the plain C and Nb steels after ferrite rolling (see Figs. 9(c) and 10(c)), although the intensities of the textures differed widely in the two steels at the beginning of  $\alpha$  rolling.

#### 4.4. Correlation between Textures and Microstructures

Another interesting point to note is the correlation between the state of the microstructure and the corresponding texture in a particular sample. Thus, quite low texture severities are observed in the plain C steel finish rolled at 1020, 870 and 730°C and also in the microalloyed steel finish rolled at 1020°C. The corresponding microstructures clearly indicate very little or no pancaking in the untransformed  $\gamma$ . By contrast, the moderately strong textures found in the Nb steel finish rolled at 870 and 730°C correlate well with the evident pancaking of a large fraction of the untransformed  $\gamma$  grains. The correlation between the most intense textures, produced by warm rolling, and the corresponding microstructures is also readily apparent.

#### 4.5. Textures and the Resultant Plastic Anisotropy

Since the plastic anisotropy of a material is very much a function of its texture, the transformation textures produced in hot and controlled rolled steels determine several industrially important mechanical properties. Figures 11(a) and 11(b) illustrate how the  $\bar{r}$ -value and yield strength are expected to vary for different texture components as a function of the angle  $\alpha$  with respect to the rolling direction.<sup>1,16)</sup> These calculations were carried out by assuming that each texture component is the only one present (with no random background), and that there is a 15° gaussian spread about the respective ideal orientation.<sup>16)</sup> In addition to the two major transformation texture components  $\{332\}\langle 113 \rangle$  and  $\{113\}\langle 110 \rangle$ , these diagrams include plots for the  $\{554\}\langle 225 \rangle$  and  $\{223\}\langle 110 \rangle$  orientations, which are derived, respectively, from the transformed Bs ( $\{332\}\langle 113 \rangle$ ) and transformed Cu ( $\{113\}\langle 110 \rangle$ ) components by warm rolling.

As can be seen from Fig. 11(a), the  $\{332\}\langle 113 \rangle$  and  $\{554\}\langle 225 \rangle$  components lead to  $\bar{r}$  values well above 2, whereas the  $\{113\}\langle 110 \rangle$  leads to  $\bar{r}$  values well below 2. Thus  $\bar{r}$  in commercial products can be influenced by the factors affecting the relative strengths of the brass and



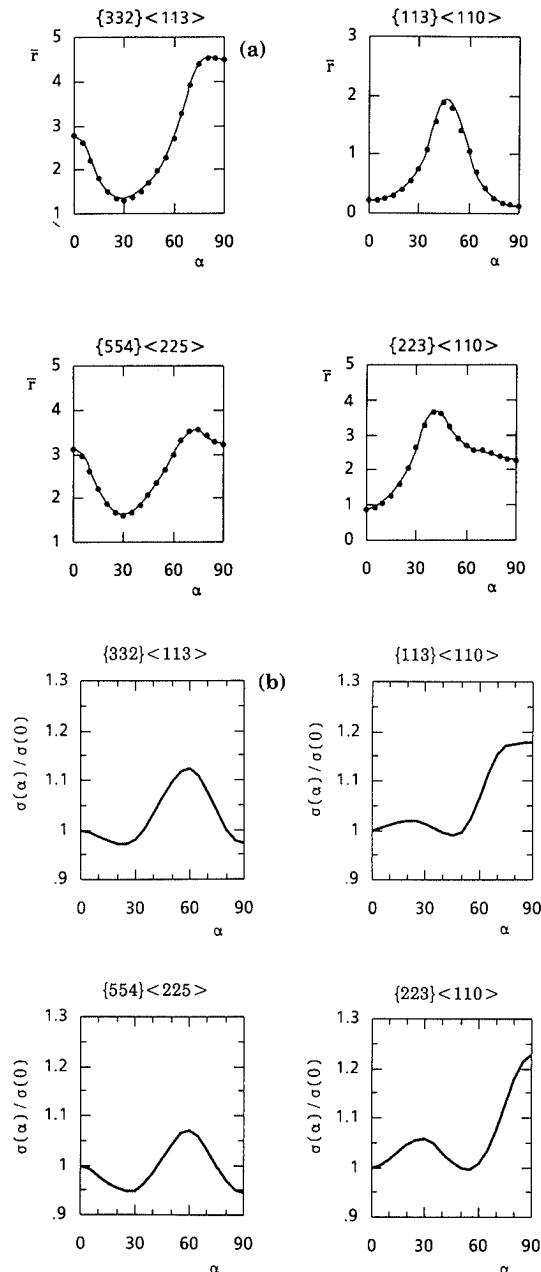


**Fig. 11.** (a) Plots of  $r$  vs. angle  $\alpha$  with respect to rolling direction for selected ideal orientations predicted by the relaxed constraint method (after Ref. 16). (b) Predictions of  $\sigma(\alpha)/\sigma(0)$  for selected texture components (after Ref. 16).

copper components in the pancaked  $\gamma$ , such as composition, austenite grain size, finish rolling temperature and cooling rate.<sup>1)</sup> In a somewhat similar manner, the ratio  $\sigma_{90}/\sigma_0$  (i.e. the transverse-to-longitudinal yield strength ratio) is also markedly influenced by the volume fractions of the  $\{113\}\langle 110\rangle$  and  $\{223\}\langle 110\rangle$  components. High proportions of the last two orientations lead to significantly higher transverse yield strengths, Fig. 11(b).<sup>16)</sup> The first of these results from the transformation of the Cu component ( $\{112\}\langle 111\rangle$ ) that is introduced by hot rolling and which is present in the pancaked (unrecrystallized) austenite. The latter is in turn formed from the  $\{113\}\langle 110\rangle$  (transformed Cu) component by the further intercritical or warm rolling

of this ferrite orientation. The strength of the Cu relative to the Bs component in the pancaked austenite is again affected by the rolling and compositional parameters described above.<sup>1)</sup>

## 5. Conclusions

(1) The plain C and Nb steel textures are similar when the steels are finish rolled in the  $\gamma$  recrystallization range (i.e. at 1020°C). The major texture components in both steels are the  $\{001\}\langle 110\rangle$  and  $\{110\}\langle 110\rangle$ , which are derived from the recrystallization texture components of the  $\gamma$ , i.e. the cube  $\{100\}\langle 001\rangle$  and its twin  $\{122\}\langle 212\rangle$ . The sharpness of the  $\{001\}\langle 110\rangle$  component generally increases with decrease in the finish rolling temperature, whereas the opposite is true for the  $\{110\}\langle 110\rangle$  component, which finally disappears after ferrite rolling.

(2) The Nb steel textures are much sharper than those of the plain C steel after finish rolling at 870 and at 730°C. The occurrence of NbCN precipitation in the microalloyed steel suppresses the recrystallization of  $\gamma$ , thereby producing a sharp  $\gamma$  rolling texture, which transforms into a well defined  $\alpha$  texture. In the plain C steel, due to the absence of Nb, no  $\gamma$  pancaking occurs and therefore only a weak  $\gamma$  texture is produced, which is inherited in diminished form by the  $\alpha$ .

(3) After finish rolling at 870°C, the other major texture components in the microalloyed steel are  $\{113\}\langle 110\rangle$  and  $\{332\}\langle 113\rangle$ , which are derived, respectively, from the  $\{112\}\langle 111\rangle$  and  $\{110\}\langle 112\rangle$  components of the unrecrystallized  $\gamma$ . A much flatter texture consisting of some broad and low intensity maxima is observed in the plain C steel.

(4) After finish rolling at 730°C, the above two texture components in the microalloyed steel are displaced to  $\{4411\}\langle 110\rangle$  and near  $\{554\}\langle 225\rangle$ . The texture of the plain C steel, although much less sharp than that of the microalloyed steel, consists of the  $\{223\}\langle 110\rangle$  and  $\{554\}\langle 225\rangle$  components, in addition to the  $\{001\}\langle 110\rangle$  and  $\{110\}\langle 110\rangle$ .

(5) Remarkably similar and sharp textures are produced in both steels by warm rolling at 630°C. The major components of the texture at this stage are the  $\{223\}\langle 110\rangle$ ,  $\{554\}\langle 225\rangle$  and  $\{001\}\langle 110\rangle$ . These are associated with well defined ND fibres.

## Acknowledgements

The authors are grateful to the Natural Sciences and Engineering Research Council of Canada (NSERC), the Canadian Steel Industry Research Association (CSIRA), and the Ministry of Education of Quebec (FCAR Program) for financial support. The extremely able secretarial help of Ms. Lorraine Mello is also gratefully acknowledged. One of the authors (M.P.B.G.) gratefully acknowledges the financial support from CONACyT, Mexico.

## REFERENCES

- 1) R. K. Ray and J. J. Jonas: *Int. Mater. Rev.*, **35** (1990), 1.
- 2) H. Saitoh, K. Ushioda, T. Senuma, T. Nakamura and K. Esaka: *Proc. Int. Conf. on Physical Metallurgy of Thermomechanical*

- Processing of Steels and Other Metals, Vol. 2, ISIJ, Tokyo, (1988), 628.
- 3) T. Senuma and H. Yada: Proc. Int. Conf. on Physical Metallurgy of Thermomechanical Processing of Steels and Other Metals, Vol. 2, ISIJ, Tokyo, (1988), 636.
  - 4) T. Nakamura and K. Esaka: Proc. Int. Conf. on Physical Metallurgy of Thermomechanical Processing of Steels and Other Metals, Vol. 2, ISIJ, Tokyo, (1988), 644.
  - 5) S. Hashimoto, T. Yakushiji, T. Kashima and K. Hosomi: Proc. Int. Conf. on Physical Metallurgy of Thermomechanical Processing of Steels and Other Metals, Vol. 2, ISIJ, Tokyo, (1988), 652.
  - 6) S. Hashimoto, T. Yakushiji, T. Kashima and K. Hosomi: Proc. 8th Int. Conf. on Textures of Materials, The Metall. Soc. of AIME, Warrendale, PA, (1988), 673.
  - 7) H. Inagaki: Proc. 5th Int. Conf. on Textures of Materials, Vol. 2, Springer-Verlag, Berlin, (1978), 157.
  - 8) H. Inagaki: Proc. 6th Int. Conf. on Textures of Materials, Vol. I, ISIJ, Tokyo, (1981), 149.
  - 9) H. Inagaki: *Z. Metallkd.*, **74** (1983), 716.
  - 10) L. Seidal, M. Hölscher and K. Lücke: *Textures Microstruct.*, **11** (1989), 171.
  - 11) R. K. Ray, Ph. Chapellier and J. J. Jonas: *Textures Microstruct.*, **12** (1990), 141.
  - 12) Ph. Chapellier: Prediction of Transformation Textures in Steels, M. Eng. Thesis, Department of Metallurgical Engineering, McGill University, Montreal, Canada, (1989).
  - 13) H. Inagaki and T. Suda: *Texture*, **1** (1972), 129.
  - 14) U. von Schlippenbach, F. Emren and K. Lücke: *Acta Metall.*, **34** (1986), 1289.
  - 15) L. S. Tóth, J. J. Jonas, D. Daniel and R. K. Ray: *Metall. Trans.*, **21A** (1990), 2985.
  - 16) D. Daniel, McGill University: Private communication.